

## Large deviations from the Clausius-Mossotti equation in a model microemulsion

M.E. Edwards, Y.H. Hwang, and X-l. Wu

*Department of Physics and Astronomy, University of Pittsburgh, Pittsburgh, Pennsylvania 15260*

(Received 7 October 1993)

We report experimental measurements of the Kerr coefficient in a model three-component microemulsion. Our measurements show that domains of the dispersed phase are strongly correlated, even for moderate to low concentrations of the dispersed phase. Such a correlation invalidates the use of the Clausius-Mossotti equation, which has been a common practice in the interpretation of light-scattering and birefringence data.

PACS number(s): 82.70.Kj, 78.20.Fm, 83.70.Hq

Certain fluids become optically birefringent when subjected to an external electric field. The effect becomes particularly significant in complex fluids, such as polymers, microemulsions, and liquid crystals, and has been used widely for studying structures and dynamics of these complex systems [1-3]. In this paper we report Kerr coefficient measurements in a three-component model microemulsion, consisting water, oil, and a surfactant. The Kerr coefficient  $K$ , as a function of molar ratio between water and the surfactant  $\omega$ , exhibits certain universal behaviors that are independent of the oil and the concentrations  $\phi$  of the dispersed phase. In particular, a scaling behavior,  $K(\phi, \omega) = \phi^2 K^*(\omega)$ , was found over a broad range of experimental parameters  $\phi$  and  $\omega$ . Here, the scaling function  $K^*(\omega)$  has a strongly nonlinear dependence on  $\omega$ , with  $K^* \sim -(\omega/\omega_0)^2$  for  $\omega/\omega_0 \rightarrow 0$  and  $\sim (\omega/\omega_0)^5$  for  $\omega/\omega_0 \gg 1$ . The  $K^*$  reaches a minimum at  $\omega_0 \sim 10$  for all concentrations,  $3.75\% < \phi < 30\%$ , used in the experiment. We noted that the scaling behavior,  $K \sim \phi^2$ , is incompatible with the Clausius-Mossotti equation (CM) which predicts that  $K \sim \phi$ . The departure from the CM equation suggests the existence of a correlation between the domains of the dispersed phase. It is surprising that such a correlation persists even at low concentrations of dispersed phase, and its effect seems to overshadow the single-particle contribution in the Kerr coefficient measurements.

The usual starting point for calculating the optical anisotropy is to write the Clausius-Mossotti equation, which relates the dielectric constant  $\epsilon (= n^2)$  to the optical polarizability  $\bar{\alpha}$  of the media [4, 5],

$$\frac{n^2 - n_s^2}{n^2 + 2n_s^2} = \frac{1}{3n_s^2} \bar{\alpha} \rho. \quad (1)$$

Here  $n_s$  and  $n$  are the zero-field indices of refraction of the solvent and the combined system of solvent plus solute, and  $\rho$  is the density of the dispersed phase. The applied external field  $\vec{E}$  breaks the rotational symmetry of the media, resulting in birefringence, which can be calculated using Eq. (1):

$$n_{\parallel} - n_{\perp} = \frac{1}{2n} \left( \frac{n^2 + 2n_s^2}{3n_s^2} \right) (\bar{\alpha}_{\parallel} - \bar{\alpha}_{\perp}) \rho, \quad (2)$$

where  $\parallel$  and  $\perp$  indicate the components that are parallel and perpendicular to the  $E$  field. For a small concentration (or density),  $n \simeq n_s + \frac{\delta n}{\delta \rho} \rho$ , we find

$$n_{\parallel} - n_{\perp} = \frac{1}{2n_s} \left( 1 + \frac{1}{3n_s} \frac{\delta n}{\delta \rho} \rho \right) (\bar{\alpha}_{\parallel} - \bar{\alpha}_{\perp}) \rho. \quad (3)$$

As can be seen, for a dilute solution with the indices of refraction of the solute and solvent that are closely matched, such as ours [6],  $\frac{1}{n_s} \frac{\delta n}{\delta \rho} \rho \ll 1$ . It follows, therefore, that the dominant contribution to the Kerr coefficient should scale linearly with  $\rho$ , and hence  $\sim \phi$ , as expected for a noninteracting system. As has already been pointed out, our very observation of  $\phi^2$  scaling in the low concentration regime violates this simple physical picture. It appears that an understanding of complex functional form of  $K^*(\omega)$  requires taking fully into account correlation between the domains of the dispersed phase [7]. Such a correlation is likely due to clustering of dispersed domains and may be further enhanced by long-range dipole-dipole interactions induced in the  $E$  field.

The system under investigation is a well-studied microemulsion, consisting of decane (oil), sodium di-ethylhexyl sulfosuccinate (AOT surfactant), and water. There are extensive scattering data in the literature, which indicates that the dispersed phase forms spherical droplets at low to moderate concentrations [8]. The size of the microemulsion droplets is of the order of 10 to 100 Å, depending on the concentration of water. However, the morphology of the microemulsion at high concentrations ( $\phi > 60\%$ ) is much less well known. Small-angle neutron scattering measurements further indicate that the microemulsion droplet is unstable upon dilution to  $\phi \leq 1\%$  [9]. In this case the system experiences a phase separation as signified by precipitation of water from the microemulsion phase. The transition from a single-phase water-in-oil microemulsion to a water-oil coexisting phase is known as emulsification failure.

Both the oil and the surfactant were purchased from Aldrich Chemical Company and were used without further purification. Double distilled and deionized water was used, which has the electric conductivity,  $\sigma < 10^{-5} \Omega^{-1} \text{m}^{-1}$ . In our experiment, systematic measurements were carried out following a set of trajectories with

the weight fraction  $\phi$ , ranging from 3.75% to 30%, being fixed while  $\omega$  was varied from 0 to  $\sim 40$ . Assuming that all the surfactant molecules stay on the water-oil interface,  $\omega$  essentially measures the volume-to-surface ratio of the dispersed phase. For a spherical microemulsion  $\omega$  is proportional to  $R$ , the radius of the droplets. The prepared samples were homogenized by stirring, using a magnetic stirring bar and by hand shaking. Additional mixing was provided prior to the measurements.

In the electric birefringence measurements a series of rectangular pulses is applied to the microemulsion. The details of the experimental setup will be published elsewhere. The pulses were generated by a Velonex high-voltage power supply with a variable pulse width,  $10^{-6} < \Delta t < 3 \times 10^{-2}$  s, and a variable pulse height,  $0 < V < 5000$  V. A horizontal electric field was applied using two stainless-steel electrodes separated by a distance  $d = 0.2$  cm. Since the separation  $d$  is much less than the width of the electrodes  $L = 1$  cm, the field inside the electrodes is uniform, and a field strength up to  $\sim 10^4$  V/cm is easily obtainable. A weakly focused He-Ne laser beam passed through an optical train, which consisted of a linear polarizer, the sample cell, a quarter-wave ( $\lambda/4$ ) plate, and an analyzer. The optical axes of the polarizer and the ( $\lambda/4$ ) plate were set at  $45^\circ$  with respect to  $\vec{E}$ , and the analyzer was set at  $90^\circ - \alpha$  with respect to the polarizer. Using the method of Jones's matrix [10], the transmitted light intensity at the detector can be calculated, with the result,

$$I = I_0 \sin^2(\pi \Delta n L / \lambda + \alpha), \quad (4)$$

where  $I_0$  is the input laser intensity,  $\lambda = 0.633 \mu\text{m}$  is the wavelength, and the birefringence  $\Delta n (= n_{\parallel} - n_{\perp})$  is the difference in the refractive indices parallel and perpendicular to  $\vec{E}$ . The use of the  $\lambda/4$  plate allows the phase angle  $\alpha$  to be varied continuously, which is useful for distinguishing the sign of birefringence  $\Delta n$ , and in increasing the sensitivity of the measurements. For  $\pi \Delta n L / \lambda \ll \alpha \ll 1$ ,  $I$  is linearly proportional to  $\Delta n$ ,

$$I \simeq I_0(\alpha^2 + 2\pi \Delta n \alpha L / \lambda). \quad (5)$$

Prior to the measurements,  $I_0$  was calibrated independently for each solution with  $\vec{E} = \vec{0}$  ( $\Delta n = 0$ ), while the angle  $\alpha$  was varied. The  $I_0$  was found by fitting the quadratic equation  $I = I_0 \alpha^2$  to the measured calibration curve. In the Kerr coefficient measurements,  $\alpha$  ranging from  $2^\circ$  to  $10^\circ$  was kept fixed depending on the signal level.

To improve the signal-to-noise ratio, a series of pulses with duty cycles less than 0.5% was applied, and the transmitted light intensity was signal averaged using a digital oscilloscope (Model HP-54600A). For certain samples, particularly those with large  $\phi$  and  $\omega$ , hydrodynamic convections due to the Joule heating were observed when a large number of pulses were applied. Accompanying the hydrodynamic convections, the birefringence signal decreased with time, presumably as a result of changing structures of the microemulsion. For this reason the number of pulses applied to the sample were kept minimal so that there would be no observable deterioration in

the optical signal during the measurements. Fortunately, for microemulsions with large  $\phi$  and  $\omega$ , the signal is so strong that even a couple of pulses are sufficient to have an accurate determination of  $\Delta n$ .

Figure 1 shows the optical transmittance,  $\Delta I = I - \alpha^2 I_0$ , as a function of  $E^2$  for a series of samples with fixed  $\phi (= 10\%)$ , but with  $\omega$  as a variable. The transmittance shown in Fig. 1 has been properly normalized by  $\alpha I_0 k_0 L$  according to Eq. (5), where  $k_0 = 2\pi/\lambda$  is the input wave number. As can be seen, in all the cases ( $10 < \omega < 40$ ),  $\Delta I$  is a linear function of  $E^2$ , even for an  $E$  field as large as  $8 \times 10^5$  V/m. The  $E^2$  dependence suggests that the measurements are well within the linear (or Kerr) regime and the optical anisotropy is essentially due to field-induced dipoles in the microemulsions. We also noted that the slope of  $\Delta I$  changes continuously from negative values to positive values as  $\omega$  increases, crossing zero at  $\omega \simeq 24$ . From the slope of these measurements, the Kerr coefficient,  $K \equiv \Delta n / E^2$ , was derived for each value of  $\omega$ .

Shown in Fig. 2 are the Kerr coefficient measurements for eight different concentrations, ranging from  $3.75\% < \phi < 30\%$ . We noted that even though  $\phi$  was varied by less than one decade,  $K$  nevertheless changes by more than two orders of magnitude. The relationship between  $K$  and  $\phi$  is not linear even for the low concentrations used in the experiment. Considering the fact that emulsification failure occurs at  $\phi \simeq 1\%$  for our system [9], the linear  $\phi$  dependence will be restricted to a very narrow concentration regime, i.e.,  $1\% < \phi < 4\%$ , if it exists at all. We also noted that, despite orders of magnitude change in  $\Delta n$ , along constant trajectories of  $\phi$ ,  $K$  exhibits interesting characteristics that are identical to all the concentrations. Namely, all the curves start from  $K = 0$  at  $\omega = 0$ , and become progressively more negative as  $\omega$  increases, reaching a minimum at approximately  $\omega \simeq 10$ . After this point,  $K$  begins to increase, yielding zero at  $\omega \simeq 24$ . By further increasing  $\omega$ ,  $K$

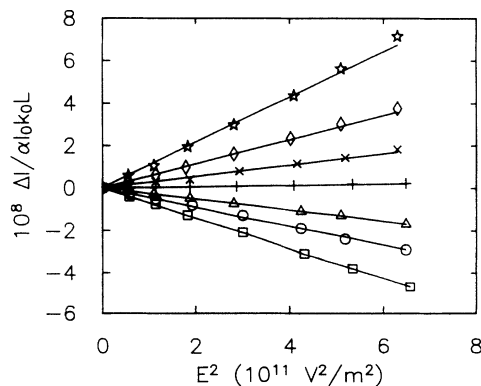


FIG. 1. The  $E^2$  dependence of electric birefringence. The measurements are for samples with  $\phi = 10\%$  and  $\omega = 10, 16, 20, 24, 26, 28,$  and  $30$ , respectively. As can be seen, as  $\omega$  increases, the slope of the normalized transmittances changes from negative to positive. Furthermore, for all values of  $\omega$ , the normalized transmittances are linear functions of  $E^2$ , indicating that the measurements are in the linear Kerr regime.

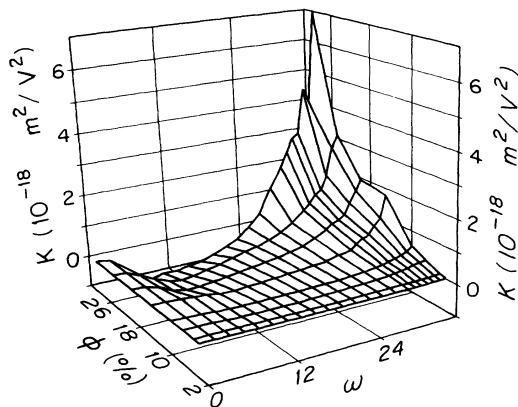


FIG. 2. Kerr coefficient  $K$  vs  $\phi$  and  $\omega$ . Along constant  $\phi$  trajectories, the Kerr coefficient decreases, passes a minimum at  $\omega_0 \simeq 10$ , and then increases monotonically as  $\omega$  increases. The Kerr coefficients decrease by more than two orders of magnitude as  $\phi$  varies from 30% to 3.75%.

becomes a rapidly increasing function of  $\omega$ . Our measurements further indicate (not shown in the figure) that for  $\phi > 30\%$ ,  $K$  appears to bend down for large  $\omega$ , giving rise to a broad peak in the Kerr-coefficient plot (Fig. 2). In this high-concentration regime, the microemulsions exhibit interesting viscoelastic behaviors, suggesting that the dispersed phase may form percolated structures with random interfaces partitioning the water and the oil phases.

The similarity in the functional dependence of  $K$  vs  $\omega$  inspired us to search for a scaling relation between  $K$  and  $\phi$ . As shown in Fig. 3, such a scaling relation does indeed exist. Here, the Kerr coefficients along a fixed  $\phi$  were normalized by a constant *prefactor*, i.e.,  $K^* = K(\phi = \text{const}, \omega) / \text{prefactor}$ , with the requirement that all the measurements with different  $\phi$  be collapsed onto a universal curve. Within the experimental uncertainties, which are typically of the order of 15%, an excellent scaling behavior was found for all the data spanning

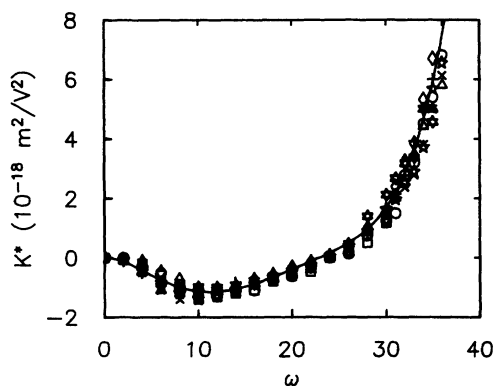


FIG. 3. Scaling form of Kerr coefficient  $K^*$ . The data are taken directly from Fig. 2, where squares, circles, triangles, pluses, diamonds, crosses, stars, and hexagons correspond to  $\phi = 3.75, 5, 7.5, 10, 15, 20, 25$ , and 30%, respectively. The solid line is a polynomial fit according to Eq. (6).

the entire concentration range between 3.75% and 30%. Plotting the *prefactor* as a function of  $\phi$ , we found that the *prefactor* increases markedly with  $\phi$  and appears to obey a quadratic form, as shown in Fig. 4. Here, the error bars are statistical errors determined by the noise in the Kerr coefficient measurements, and the solid line is a quadratic fit to the data.

Our experiment, therefore, suggests that  $K(\phi, \omega) \sim \phi^2 K^*(\omega/\phi^x)$  with the scaling function,  $K^*(\omega/\phi^x)$ , nearly independent of  $\phi$ , i.e.,  $x = 0$ . Careful inspection of Fig. 3 further suggests that for small values of  $\omega$  ( $\omega \ll \omega_0 = 10$ ),  $K^* \sim -(\omega/\omega_0)^2$ , whereas for large  $\omega$  ( $\omega \gg \omega_0$ ),  $K^* \sim (\omega/\omega_0)^\sigma$  with  $\sigma > 3$ . Fitting the scaling function using a polynomial of the form,

$$K^* = \sum_2^\sigma C_m (\omega/\omega_0)^m, \quad (6)$$

and slowly incrementing  $\sigma$ , we found that the lowest order polynomial that still mimics satisfactorily the experimental data corresponds to  $\sigma = 5$ . The coefficients, as a result of such a fitting procedure, are given by  $C_2 = -4.33 \times 10^{-18}$ ,  $C_3 = 4.74 \times 10^{-18}$ ,  $C_4 = -1.77 \times 10^{-18}$ , and  $C_5 = 2.32 \times 10^{-19}$ , and they all have the dimension of  $m^2/V^2$ . The fitting curve is shown as a solid line in Fig. 3, and it is evident from the graph that the quality of the fit is excellent. We noted that all the coefficients are approximately the same order of magnitude. Reducing the number of fitting parameters, either at the lower or at the higher ends of the polynomial, significantly reduces the quality of the fit. On the other hand, increasing the number of terms in the polynomial only improves the fit slightly with the extra fitting parameters being so small that they are essentially negligible. It should be pointed out that the general behavior of  $K^*$  appears to be quite universal, independent of the oil used. For instance, replacing decane by decalin produces essentially the same functional dependence of  $K^*$  on  $\omega$ , with  $\omega_0 \sim 7$ . Similar behavior has also been reported for iso-octane [4].

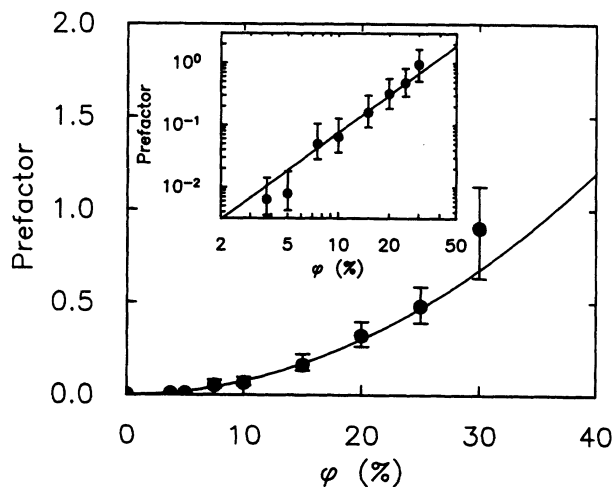


FIG. 4. The *prefactor* vs concentration  $\phi$ . The solid circles are determined from the experimental data by imposing the scaling condition for the Kerr coefficients. The solid line is a quadratic fit,  $\text{prefactor} \sim \phi^2$ . The inset is the log-log plot of the same graph.

What are the mechanisms for the Kerr coefficient to display such a complex, nonlinear dependence on  $\omega$ ? It has been suggested by several authors [4, 5, 11] that the complex relationship between  $K$  and  $\omega$  is a result of deformation of individual microemulsion droplets in an external  $E$  field. The single-droplet theory depicts the negative  $K$  as arising from the anisotropy of the AOT molecule that are aligned with the electric field by their permanent dipole moments. The negative  $K$  of each AOT molecule results from the polarizabilities being greater perpendicular to than parallel to the electric field. The core portion of the droplet produces positive  $K$  that is due to the elongation of the particles into spheroids, with the long axis parallel to the  $E$  field. For small  $\omega$ , the AOT monolayer on the oil-water interface has the dominant contribution to the Kerr coefficient, giving rise to a negative, intrinsic birefringence. On the other hand, as the water core gets larger, with increasing  $\omega$ , the core contribution becomes more significant, yielding a positive, form birefringence. The competition between the intrinsic and the form birefringences, therefore, gives  $K$ , which passes a minimum at a negative value and subsequently becomes positive as  $\omega$  increases.

Within the single-droplet approximation, the electric birefringence  $\Delta n = n_{\parallel} - n_{\perp}$  can be calculated using the CM equation, taking into account the elastic deformation of the microemulsion droplets. To illustrate the main idea behind the calculation and to obtain a qualitative result, we repeat the derivation using Eq. (3) and a simple dimensional analysis. In the linear response regime,  $\Delta n$  is proportional to both the low-frequency (dc) and the high frequency (ac) polarizabilities of the fluid, where the dc part couples to the applied external electric field while the ac part couples to the probing electromagnetic waves, the laser light in this case. It is further assumed that both the dc and the ac polarizabilities are linear combinations of a term from the water-core ( $\alpha_W$ ) and a term from the surfactant layer on the interface ( $\alpha_S$ ), where  $\alpha_i$  stands for molecular polarizability of the corresponding component  $i$ . This yields

$$n_{\parallel} - n_{\perp} \sim \left( \frac{4\pi}{3} R_w^3 \alpha_W(ac) + 4\pi d R_w^2 \alpha_S(ac) \right) \times \left( \frac{4\pi}{3} R_w^3 \alpha_W(dc) + 4\pi d R_w^2 \alpha_S(dc) \right) E^2 \rho, \quad (7)$$

where  $R_w$  is the water-core radius of the microemulsion droplets and  $d$  is the interfacial thickness, which is approximately the length of a surfactant molecule. Since  $\rho \sim \phi/R_w^3$ , Eq.(7) predicts that (1)  $\Delta n$  is linearly proportional to  $\rho$ , hence  $\sim \phi$  at low concentrations; (2)  $\Delta n$  is proportional to  $E^2$ , as expected for spherical droplets with inversion symmetry in the  $E$  field; and (3)  $\Delta n$  is a polynomial of  $R_w$  with the leading term  $\sim R_w^3$  and the lowest-order term  $\sim R_w$ . For  $R_w \gg d$  and assuming that all the surfactants stay on the interface, we have  $R_w \sim \omega$  (=volume/surface). Therefore, the single-droplet model predicts that  $\Delta n$  scales with  $\omega$  as  $\Delta n \sim A_3\omega^3 + A_2\omega^2 + A_1\omega$ . Detailed calculations [4], using appropriate dielectric constants for various constituents, further indicate that  $A_1$  and  $A_2$  are negative constants,

while  $A_3$  is a positive constant. Namely, the competition between the form birefringence due to the water core and the intrinsic birefringence due to the surfactant layer can give rise to a minimum in  $K$  ( $< 0$ ) similar to that shown in Fig. 3. Using the above theory, the bending elastic constant of AOT microemulsion was found to be  $\sim 0.5k_B T$  in several different oils.

Our measurements differ from the above single-droplet picture in several important ways. Most notably is the  $\phi^2$  dependence for both the small and the large values of  $\omega$ , corresponding to regimes of negative and positive birefringence. In the single-droplet model the negative part of the Kerr coefficient can only result from intrinsic birefringence and, therefore, it scales linearly with  $\phi$ . Furthermore, in our experiment the leading term of  $\Delta n$  is  $\sim \omega^5$ , instead of  $\omega^3$ , as predicted by the single-droplet model. We were not able to fit our experimental data using polynomials of order less than 5. Likewise, the lowest-order term in our fitting procedure appears to be  $\sim \omega^2$ , instead of  $\omega$ . If the linear term is included in the fitting using Eq. (6), a small negative number is obtained, with  $C_1 = -4.7 \times 10^{-20}$ , which is negligible as compared to the other terms, as mentioned above. The most significant observation of the experiment is the  $\phi^2$  dependence, which appears to persist for concentrations as low as a few percent. Since the microemulsion is no longer stable for  $\phi \leq 1\%$ , our experiment suggests that the linear  $\phi$ -dependent regime would be restricted to a very narrow concentration range if it still exists. A conspicuous similarity for the Kerr coefficients  $K(\phi, \omega)$  along different concentration trajectories further suggests that the mechanism which gives rise to the complex  $\omega$  dependence,  $K^*(\omega)$ , is essentially the same in both the low- and the high-concentration regimes.

In conclusion, our measurements of the Kerr coefficient in a model microemulsion show significant deviations from the Clausius-Mossotti equation over a broad range of parameters, including low-concentration regimes,  $\sim 4\%$ , where such an equation is expected to be valid. The experiment calls for a need to find a new mechanism that will give the correct scaling behaviors observed in the experiment. It appears that such a mechanism must incorporate correlation between various constituents, such as domain-domain and domain-interface correlation, even at low concentrations. It will also be useful to examine the transient behaviors of the electric birefringence signal after switching on and off the  $E$  field. Our preliminary measurements indicate that the characteristic relaxation time  $\tau$  after switching off the field scales linearly with  $\omega$ , which is again in disagreement with the single-droplet model which predicts  $\tau \sim \omega^3$  if the relaxation is determined by the bending elasticity of the surfactant membrane. Detailed studies of the time-dependent electric birefringence are currently underway and will be published elsewhere.

We would like to thank Walter Goldberg, J.S. Huang, S. Milner, Ari Shinozaki, and Chuck Yeung for many useful discussions. This research is partially supported by the American Chemical Society under Grant No. PRF 26567-AC9, and the National Institutes of Health under Grant No. GM08206.

- [1] M. Doi and S.F. Edwards, *Polymer Dynamics* (Clarendon, Oxford, 1986).
- [2] X-l. Wu, C. Yeung, M.W. Kim, J.S. Huang, and D. Ouyang, *Phys. Rev. Lett.* **68**, 1426 (1992).
- [3] M.K. Hong, O. Narayan, R.E. Goldstein, E. Shyamsunder, R.H. Austin, D.S. Fisher, and M. Hogan, *Phys. Rev. Lett.* **68**, 1430 (1992).
- [4] E. Van der Linden, S. Geiger, and D. Bedeaux, *Physica A* **156**, 130 (1989).
- [5] M. Borkovec and H.F. Eicke, *Chem. Phys. Lett.* **157**, 457 (1989).
- [6] The term  $\frac{1}{n} \frac{\delta n}{\delta \phi} \phi$  amounts to a few percent correction to Eq. (3), even in the most unfavorable cases. Therefore it is negligible in our experiment.
- [7] A. Onuki and M. Doi, *Europhys. Lett.* **17**, 63 (1992).
- [8] S.H. Chen, T.L. Lin, and J.S. Huang, *Physics of Complex and Supermolecular Fluids*, edited by S.A. Safran and N.A. Clark (Wiley, New York, 1987), pp. 285–313; M. Kotlarchyk, S.H. Chen, J.S. Huang, and M.W. Kim, *Phys. Rev. A* **29**, 2054 (1984).
- [9] X-l. Wu, P. Tong, and J.S. Huang, *J. Colloid Interface Sci.* **148**, 104 (1992).
- [10] A. Yariv and P. Yeh, *Optical Waves in Crystals* (Wiley, New York, 1984).
- [11] R. Hilfiker, H.F. Eicke, and H. Hammerich, *Helv. Chim. Acta* **70**, 1531 (1987).